frontiers | Frontiers in Materials

ORIGINAL RESEARCH
published: 18 May 2022
doi: 10.3389/fmats.2022.897900

Effect of PyC Inner Coating on Preparation of 3C-SiC Coating on Quartz Glass by Chemical Vapor Reaction

Jian Wu[1,2,3], *Shengteng Qian*[1,3], *Tongguo Huo*[1,3], *Jianxin Zheng*[1,3], *Pinlong Zhang*[1,3], *Yu Dai*[1,2,3]* and *Dongsheng Geng*[4]*

[1]School of Physics and Materials, Nanchang University, Nanchang, China, [2]International Institute of Materials Innovation, Nanchang University, Nanchang, China, [3]Hunan Advanced Corporation for Materials and Equipments, ACME, Changsha, China, [4]Beijing Advanced Innovation Center for Materials Genome Engineering, Beijing Key Laboratory for Magneto-Photoelectrical Composite and Interface Science, School of Materials Science and Engineering, University of Science and Technology Beijing, Beijing, China

OPEN ACCESS

Edited by:
Yakun Zhu,
United States Department of Energy (DOE), United States

Reviewed by:
Dachi Yang,
Nankai University, China
Shiyu Cui,
Nanchang Hangkong University, China

***Correspondence:**
Yu Dai
daiyu@vip.163.com
Dongsheng Geng
dgeng@ustb.edu.cn

Specialty section:
This article was submitted to Environmental Degradation of Materials, a section of the journal Frontiers in Materials

Received: 16 March 2022
Accepted: 29 March 2022
Published: 18 May 2022

Citation:
Wu J, Qian S, Huo T, Zheng J, Zhang P, Dai Y and Geng D (2022) Effect of PyC Inner Coating on Preparation of 3C-SiC Coating on Quartz Glass by Chemical Vapor Reaction. Front. Mater. 9:897900. doi: 10.3389/fmats.2022.897900

The cubic polycrystal of SiC (3C-SiC) coating on the quartz glass (QG) surface was successfully prepared via a two-step chemical vapor deposition (CVD) by introducing a thin PyC coating as a buffer layer. Through combining the intake system of CVD PyC and CVD SiC, the SiC/PyC composite coating can be *in-situ* prepared on the QG without halfway in-and-out chamber. The results showed that the SiC/PyC composite coating possesses highly uniform, dense, and continuous features, while the pure SiC coating exhibits many cracks, implying that the internal stress between the SiC coating and the QG can be relieved by adding the PyC buffer coating. The average hardness of the SiC/PyC/QG is measured to be 46.8 GPa, and its calculated modulus is 416.3 GPa by using a nanoindentation technique. Compared to the pure QG, the friction coefficient of the SiC/PyC/QG is slightly increased to 1.47 vs. 1.45. Moreover, the SiC/PyC/QG displays the excellent anti-acid corrosion in the 5%HF and 5%HCl mixed solution with the weight loss of about 33% lower than the pure QG after 8 h acid test at 80°C.

Keywords: SiC coating, pyc coating, quartz glass, chemical vapor deposition, anti-acid corrosion

INTRODUCTION

Quartz glass (QG) is widely used in the field of the compound semiconductor community as the boat for the growth of CdTe, InTe and CdZnTe single crystal in the field of the compound semiconductor community due to the advantage of resistance to high temperature, excellent anti-acid corrosion except hydrofluoric acid (HF), good thermal stability etc. (Rabinovich 1985; Shetty et al., 1995; Schlesinger et al., 2001; Hoshide and Hirano 2010). But the raw materials of Te and Cd would react with the QG during the single crystal growing process, resulting in the as-prepared product adhered to the QG. Thus, the single crystal would be contaminated by the QG and hard to get off the QG. Furthermore, the QG needs to be cleaned in HF to remove the sediment, while the QG shows poor anti-HF corrosion. Therefore, the QG or quartz fiber coated with a protective material has been extensively studied to improve its chemical durability and other physical properties (Shetty et al., 1995; Hoshide and Hirano 2010; Zheng and Wang 2011; Hoshide et al., 2013). The cubic polycrystal of SiC (3C-SiC) is one of the most important protective materials and drawing significant attention attributing to its high hardness and strength, good corrosion

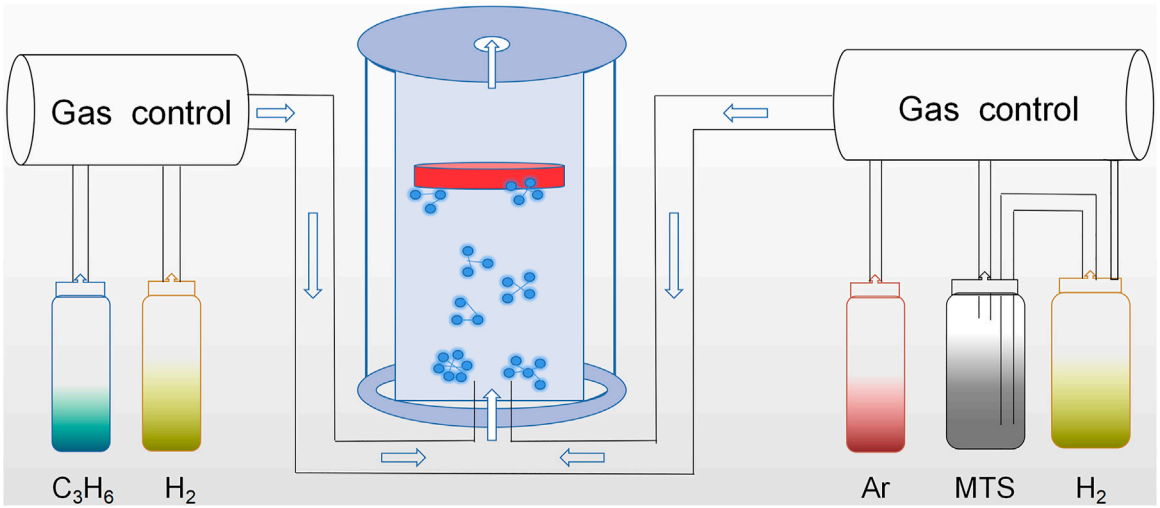

FIGURE 1 | Schematic illustration for the experimental apparatus of CVD.

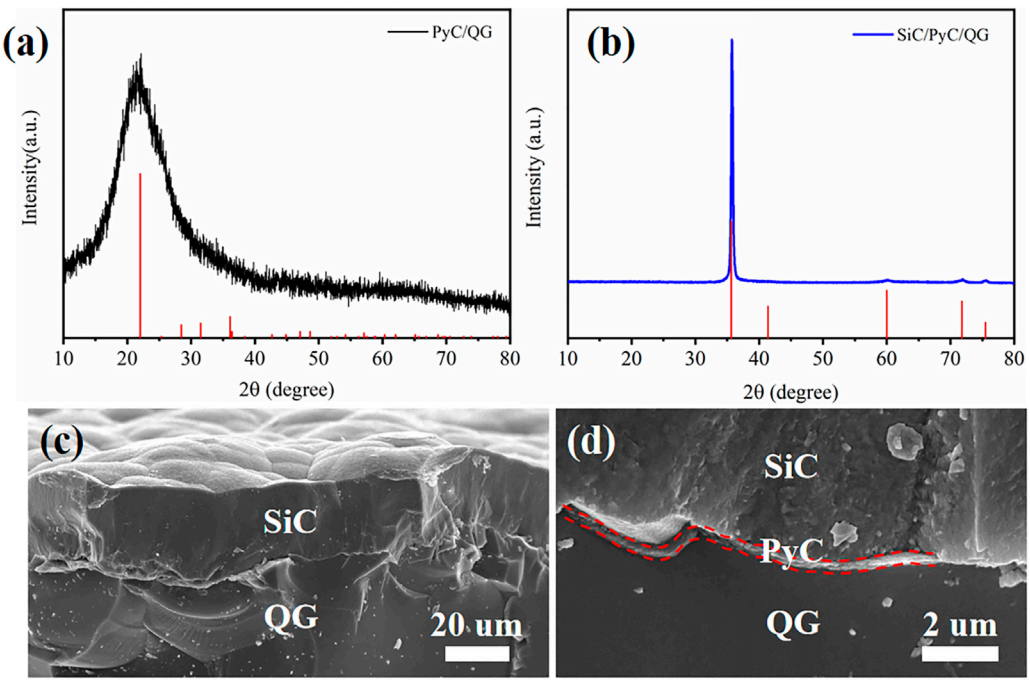

FIGURE 2 | XRD pattern of **(A)** the PyC/QG, and **(B)** the SiC/PyC/QG; **(C)** cross section of the low-magnification and **(D)** the high-magnification SEM images of the SiC/PyC/QG.

resistance, and easy of deposition (Hu et al., 2019; Fares et al., 2020a; Fares et al., 2020b; Hsu et al., 2020; Zheng et al., 2021; Liu et al., 2022a). However, to the best of our knowledge, the 3C-SiC protective coating on the QG surface is still lacking mainly due to the high internal stress and high thermal expansion coefficient mismatch between QG and SiC. The introduction of the pyrolytic carbon (PyC) as the buffer layer is widely used to alleviate thermal stress due to the interlaminar slippage of PyC and the large thermal expansion coefficient mismatch between the coating and the substrate (Long et al., 2013; Liu et al., 2020; Tong et al., 2021; Liu et al., 2022b).

In this work, it was attempted to deposit the 3C-SiC coating on the QG surface by a two-step CVD using the PyC coating as the buffer coating without halfway in-and-out chamber. In

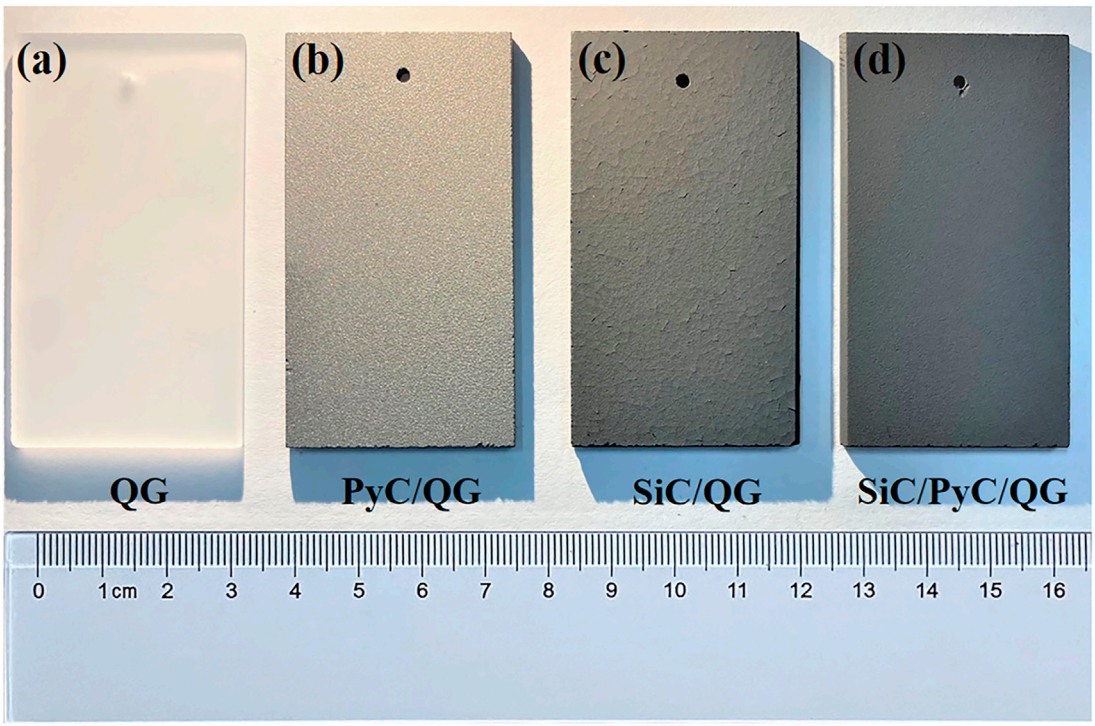

FIGURE 3 | The picture of **(A)** the QG, **(B)** the PyC/QG, **(C)** the SiC/QG, and **(D)** the SiC/PyC/QG.

comparison to the pure QG, the resulting product shows the remarkably improved hardness, modulus, friction coefficient, and the anti-acid corrosion in the 5%HF and 5%HCl mixed solution.

EXPERIMENTAL

Commercial QG (25 mm*45 mm*3 mm) was ultrasonically cleaned in ethanol and deionized water several times. The pretreated QG was dried under vacuum at 60°C for 12 h and then employed as a substrate for CVD PyC coating and CVD SiC coating in a chamber of a vertical type hot-wall CVD (Hunan Advanced Corporation for Materials and Equipments, ACME, China). The CVD PyC was deposited at 1,000°C in an Ar flow of 300 ml/min and C_3H_6 flow of 200 ml/min for 2 h under the pressure of 2000 Pa. Then, the intake system of the PyC deposition was shut down, while the temperature was kept at 1,000°C. For the CVD SiC coating, a mixture of dilution H_2 flow of 2.0 L/min and dilution Ar flow of 2.5 L/min was introduced into the chamber. Meanwhile, the liquid methyltrichlorosilane (MTS) as the Si and C source was delivered to the chamber through continuous bubbling methods with an H_2 flow of 1.0 L/min as a carrier gas. The total pressure was controlled to be 1,000 Pa, and the deposition time was 5 h. The anti-acid corrosion character of the samples was test in the mixed solution of 5%HF and 5%HCl at 80°C. The samples were submerged into the acid solution completely for each 2 hours, and then weighted after ultrasonic cleaning in deionized water and drying.

A roughness tester (TR210, Shanghai Lingyi Company, China) was used to measure the surface roughness (Ra) of the samples. X-ray diffraction (XRD, Rigaku SmartLab-SE, Japan) with Cu K_α radiation and scanning electron microscopy (SEM, Carl Zeiss G500) were carried out to characterize the crystal structure and the morphology of the products, respectively. X-ray photoelectron spectroscopy (XPS) analysis was obtained by a Thermo Fisher Scientific Esca Lab 250XI spectrometer using a monochromatic Al anode X-ray source. The mechanical properties of the samples were investigated by the conventional method (Vickers, Duramin-40 M1 Struers), the nanoindentation test with a diamond Berkovich indenter (three-sided pyramid), and the friction test on a HT1000 wear test machine with a Si_3N_4 ceramic ball was used as the counter material.

RESULTS AND DISCUSSION

The synthesis produce of the SiC/PyC/QG is illustrated in **Figure 1**. Firstly, a thin and uniform PyC coating was prepared on the QG surface via a CVD method using C_3H_6 as the carbon source. Afterwards, the SiC coating could be *in-situ* grown on the PyC/QG surface just by closing the intake system of the CVD PyC, and then turning on the intake system of the CVD SiC. Therefore, the SiC/PyC composite coating can be continually deposit on the QG surface by a two-step CVD process without halfway in-and-out chamber.

The crystallographic structure and morphology of the QG based products were investigated by XRD and SEM, respectively. The identified diffraction peaks in **Figure 2A** are indexed to the SiO_2 structure (JCPDS: 39-1425), and the wide peak around 2θ = 22° in the XRD pattern is attributed to the amorphous QG. No

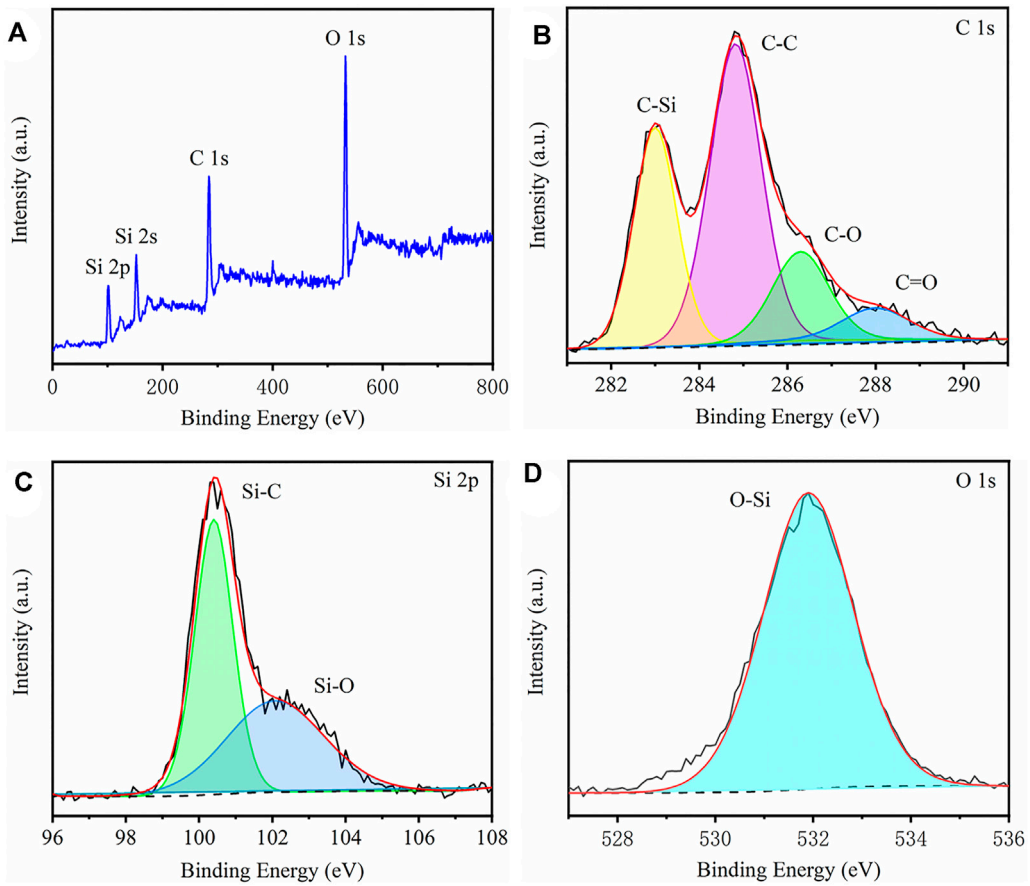

FIGURE 4 | XPS spectra of the SiC/PyC/QG: **(A)** overall spectrum; **(B)** C 1s; **(C)** Si 2p; **(D)** O 1s.

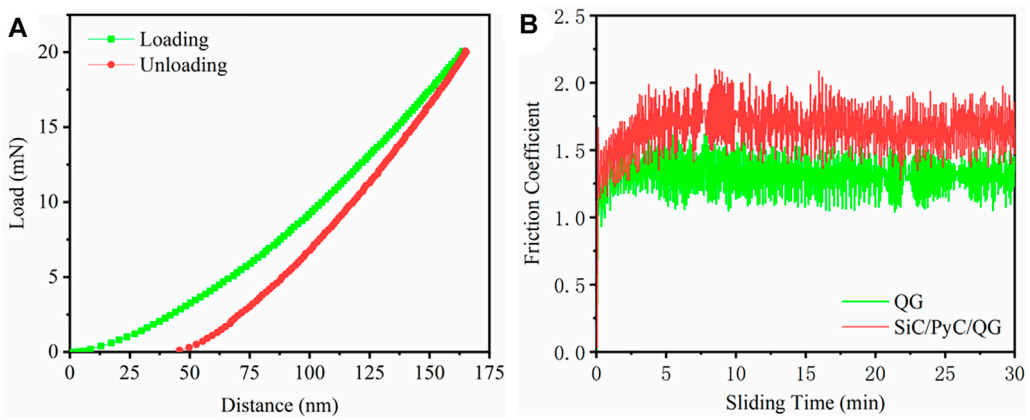

FIGURE 5 | (A) Load-distance curve of the SiC/PyC/QG; **(B)** Friction coefficient versus the sliding time (min) of the pure QG and the SiC coating'QG.

obvious peaks of the PyC could be identified owing to the strong background peaks of the QG and the thin PyC coating. The main phase of the SiC coating is ascribed to 3C-SiC (JCPDS: 29-1129), and the sharp diffraction peak demonstrates that the SiC deposits were well-crystallized (**Figure 2B**).

The SEM images of the SiC/PyC/QG are shown in **Figure 2C** and **Figure 2D**. The thickness of the PyC and SiC coatings was about 0.2 and 30 μm, respectively. It can be clearly seen that both the interfacial layers between PyC and QG, and SiC and PyC are uniform, dense, and continuous without obvious defects such as

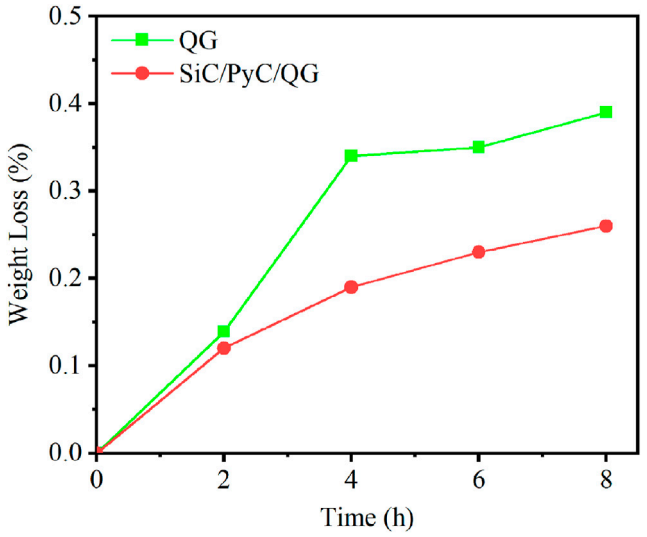

FIGURE 6 | Graph of weight loss (%) versus time (h) of the pure QG and the SiC coating'QG.

voids, cavities, and crack, implying that the interfacial adhesion was qualitatively excellent.

Figure 3A displays the typical picture of the frosted QG treated by sand blasting. The dense and continuous PyC and SiC coatings on the QG surface can be seen (**Figures 3B,D**) further revealing the uniform coatings coverage. However, many cracks appeared on the surface of the SiC coating without the PyC buffer layer (**Figure 3C**), indicating that the transition layer of PyC could relieve the internal stress between the SiC coating and the QG.

The surface chemical composition and bonding information of the SiC/PyC/QG are shown in **Figure 4**. It can be clearly seen in **Figure 4A** that the overall XPS spectrum of the as-prepared composites consists of only Si, C and O elements. The C 1s spectra (**Figure 4B**) shows four peaks located at 282.7, 284.8, 286.3 and 288.0 eV, corresponding to Si-C, C-C, C-O and C=O bonds, respectively (Zheng et al., 2021; Lu et al., 2019). The C-C bond is most likely to the PyC and the chemical bonding between SiC and PyC. Similarly, the C-O and C=O bonds may be also due to the PyC and the chemical bonding between SiC and PyC. In the Si 2p spectra (**Figure 4C**), Si 2p peak can be fitted into two peaks at 100.4 and 102.0 eV, which are assigned to the Si-C and Si-O bonds, respectively (Wei et al., 2020; Peng et al., 2018). In **Figure 4D**, O 1s spectra at 532.0 eV is assigned to the O-Si bond (Sun et al., 2017). The XPS results further confirmed the deposition of SiC coating on the PyC/QG surface.

Hardness and elastic modulus of the SiC/PyC/QG were studied by using a nanoindentation technique. The load-distance relationship is represented in **Figure 5A**, and three different points were selected to achieve a reliable result. The average hardness of the composites is 46.8 GPa, and the calculated modulus is 416.3 GPa, which are in agreement with other reported results (Lee et al., 2000). **Figure 5B** shows the variation of the friction coefficient with sliding time. Compared to the friction coefficient of the pure quartz (~1.45), the friction coefficient of the SiC/PyC/QG is increased to 1.47. The surface roughness for the PyC coating on the QG was measured to be 3.54 um. The higher friction coefficient for the SiC coating is due to the large surface roughness for the SiC coating (4.07 μm) than that of the pure QG (2.83 μm).

Figure 6 demonstrates the variation of the weight loss with the immersion time recorded for the pure QG and the SiC coated QG in the mixed solution of 5%HF and 5%HCl at 80°C. In the first 2 hours, the weight loss of the SiC/PyC/QG was 0.12%, slightly lower than that of the pure QG of 0.14%. Clearly, the weight loss of the pure QG increased to 0.34%, but the SiC coated QG displayed an excellent anti-acid corrosion with only weight loss of 0.19%. After 8 hours, the weight loss of the pure QG and the SiC/PyC/QG was 0.39% and 0.26%, respectively. The results indicated that the SiC coated QG possesses more outstanding anti-acid corrosion than the pure QG due to the unique characters of the SiC coating.

CONCLUSION

Integration of the CVD PyC and CVD SiC systems, the SiC/PyC composite coating was successfully *in-situ* prepared on the QG surface without halfway in-and-out chamber. The effects of the PyC buffer coating on the preparation of SiC coating on the QG surface were investigated. It was found that the SiC/PyC composite coating exhibited uniform, dense and continuous features by adding the PyC buffer coating, while the pure SiC coating on the QG surface displayed many cracks or even peeled off due to the high internal stress and big thermal expansion coefficient mismatch between the SiC coating and the QG. The hardness of the SiC/PyC/QG was 46.8 GPa, and its modulus was calculated to be 416.3 GPa. The friction coefficient of the SiC/PyC/QG was slightly higher than that of the pure QG with 1.47 vs. 1.45. The SiC coated QG displayed more excellent anti-acid corrosion than the pure QG in the 5%HF and 5%HCl mixed solution with the lower weight loss of 0.26% versus 0.39% after 8 h acid test.

DATA AVAILABILITY STATEMENT

The original contributions presented in the study are included in the article/Supplementary Material, further inquiries can be directed to the corresponding authors.

AUTHOR CONTRIBUTIONS

SQ: Data curation. TH: Formal analysis. JZ: Methodology. PZ: Investigation. YD, and DG: Supervision. All authors contributed to manuscript revision and read and approved the submitted versions.

FUNDING

This work has been supported by the Jiangxi Provincial Natural Science Foundation of China (No.

20192BAB216009), the Science and Technology Planning Project of Hunan Province, China (No. 2019WK 2051), and Science and Technology Project of Changsha, Hunan, China (No. kh2003023).

REFERENCES

Fares, C., Elhassani, R., Partain, J., Hsu, S. M., Craciun, V., Ren, F., et al. (2020). Annealing and N2 Plasma Treatment to Minimize Corrosion of SiC-Coated Glass-Ceramics. *Mater. (Basel)* 13, 2375–2387. doi:10.3390/ma13102375

Fares, C., Hsu, S. M., Xian, M., Xia, X., Ren, F., Mecholsky, J. J., et al. (2020). Esquivel-Upshaw, J., Demonstration of a SiC Protective Coating for Titanium Implants. *Mater. (Basel)* 13, 2375–2387. doi:10.3390/ma13153321

Hoshide, T., and Hirano, M. (2010). Evaluation of Strength for Borosilicate Glass Coated with Ceramic Materials by Sputtering. *J. Mater. Eng. Perf.* 19, 562–567. doi:10.1007/s11665-009-9520-9

Hoshide, T., Shimizu, S., and Tanaka, M. (2013). Fatigue Life Properties and Availability of Proof Testing in Ceramics-Coated Glass. *J. Mater. Eng. Per.* 23, 753–758. doi:10.1007/s11665-013-0844-0

Hsu, S. M., Ren, F., Chen, Z., Kim, M., Fares, C., Clark, A. E., et al. (2020). Novel Coating to Minimize Corrosion of Glass-Ceramics for Dental Applications. *Mater. (Basel)* 13, 1215–1225. doi:10.3390/ma13051215

Hu, Z., Zheng, D., Tu, R., Yang, M., Li, Q., Han, M., et al. (2019). Structural Controlling of Highly-Oriented Polycrystal 3C-SiC Bulks via Halide CVD. *Mater* 12, 390–399. doi:10.3390/ma12030390

Lee, K. S., Park, J. Y., Kim, W. J., Lee, M. Y., and Jung, C. H. (2000). Effect of Soft Substrate on the Indentation Damage in Silicon Carbide Deposited on Graphite. *J. Mater. Sci.* 35 (11), 2769–2777. doi:10.1023/A:1004778614890

Liu, J., Chen, Z., Chai, P., Wan, Q., and Shahzad, A. (2022). The Effect of Deposition Temperature on Microstructure and Mechanical Properties of SiC Coatings on Graphite. *J. Au. Ceram. Soc.* doi:10.1007/s41779-021-00699-7

Liu, X. L., Dai, Y., Wang, Z. J., and Wu, J. (2022). Research Progress on Tantalum Carbide Coatings on Carbon Materials. *New Carbon Mater.* 36, 1049–1061. doi:10.1016/S1872(21)60101-410.1016/j.carbon.2021.12.005

Liu, X., Xu, H., Xie, F., Yin, X., and Riedel, R. (2020). Light-Weight and Highly Flexible TaC Modified PyC Fiber Fabrics Derived from Cotton Fiber Textile with Excellent Electromagnetic Shielding Effectiveness. *Chem. Eng. J.* 387, 124085–104098. doi:10.1016/j.cej.2020.124085

Long, Y., Javed, A., Zhao, Y., Chen, Z. K., Xiong, X., and Xiao, P. (2013). Fiber/matrix Interfacial Shear Strength of C/C Composites with PyC–TaC–PyC and PyC–SiC–TaC–PyC Multi-Interlayers. *Ceram. Inter.* 39, 6489–6496. doi:10.1016/j.ceramint.2013.01.080

Lu, W., Tarekegne, A. T., Ou, Y., Kamiyama, S., and Ou, H. (2019). Temperature-dependent Photoluminescence Properties of Porous Fluorescent SiC. *Sci. Rep.* 9, 16333–163342. doi:10.1038/s41598-019-52871-6

Peng, Y., Pan, N., Wang, D., Yang, J., Guo, Z., and Yuan, W. (2018). A Si–O–Si Bridge Assembled from 3-mercaptopropyltrimethoxysilane and Silicon Carbide for Effective Charge Transfer in Photocatalysis. *J. Mater. Sci.* 53, 12432–12440. doi:10.1007/s10853-018-2518-7

Rabinovich, E. M. (1985). Preparation of Glass by Sintering. *J. Mater. Sci.* 20, 4259–4297. doi:10.1007/BF00559317

Schlesinger, T. E., Toney, J. E., Yoon, H., Lee, E. Y., Brunett, B. A., and Franks, L. (2001). Cadmium Zinc telluride and its Use as a Nuclear Radiation Detector Material. *Mater. Sci. Eng.* 32, 103–189. doi:10.1016/S0927-796X(01)00027-4

Shetty, R., Wilcox, W. R., and Regel, L. L. (1995). Influence of Ampoule Coatings on Cadmium telluride Solidification. *J. Cryst. Growth* 153, 103–109. doi:10.1016/0022-0248(95)00149-2

Sun, X., Liu, H. T., and Cheng, H. F. (2017). Oxidation Behavior of Silicon Nitride Fibers Obtained from Polycarbosilane Fibers via Electron Beam Irradiation Curing. *RSC Adv.* 7, 47833–47839. doi:10.1039/c7ra09056k

Tong, M., Fu, Q., Liang, M., Feng, T., Hou, W., Sun, J., et al. (2021). Effect of PyC-SiC Double-Layer Interface on Ablation Behaviour of Impacted CVD-SiCnws/HfC Coating. *Corros. Sci.* 191, 109741–109752. doi:10.1016/j.corsci.2021.109741

Wei, J., Li, X., Wang, Y., Chen, B., Zhang, M., and Qin, C. (2020). Photoluminescence Property of Inexpensive Flexible SiC Nanowires Membrane by Electrospinning and Carbothermal Reduction. *J. Am. Ceram. Soc.* 103, 6187–6197. doi:10.1111/jace.17396

Zheng, X., Liu, Y., Fu, S., Cao, Y., and Zhang, Y. (2021). Effect of Deposition Temperature and Time on Microstructure of CVD SiC Coating on diamond Particles. *Sur. Inter.* 24, 109741–109752. doi:10.1016/j.surfin.2021.101076

Zheng, Y., and Wang, S. (2011). Synthesis of boron Nitride Coatings on Quartz Fibers: Thickness Control and Mechanism Research. *Appl. Surf. Sci.* 257, 10752–10757. doi:10.1016/j.apsusc.2011.07.092

Conflict of Interest: The authors declare that the research was conducted in the absence of any commercial or financial relationships that could be construed as a potential conflict of interest.

Publisher's Note: All claims expressed in this article are solely those of the authors and do not necessarily represent those of their affiliated organizations, or those of the publisher, the editors and the reviewers. Any product that may be evaluated in this article, or claim that may be made by its manufacturer, is not guaranteed or endorsed by the publisher.